Spectroscopic and photophysical study of an anthryl probe: DNA binding and chiral recognition

Abdel R. Al Rabaa,[a] Francis Tfibel,[a] Fabienne Mérola,[b] Pascal Pernot[c] and Marie-Pierre Fontaine-Aupart*[a]

[a] *Laboratoire de Photophysique Moléculaire, UPR 3361 CNRS, Université Paris-Sud, 91405 Orsay cedex, France*
[b] *LURE, Université Paris-Sud, BP 34, 91898 Orsay cedex, France*
[c] *Laboratoire de Physico-Chimie des Rayonnements, UA 75 CNRS, Université Paris Sud, 91405 Orsay cedex, France*

Received (in Cambridge) 24th June 1998, Accepted 4th December 1998

Binding of Pirkle's acid (2,2,2-trifluoro-1-(9-anthryl)ethanol; TFAE) to different double stranded polynucleotides namely poly(dA-dT)-(dA-dT), poly(dG-dC)-poly(dG-dC) and calf thymus DNA, was examined for the first time by following changes in the photophysical properties of each enantiomer of the chromophore using steady state as well as time resolved absorption and fluorescence methods. The observed effects on absorption, fluorescence quantum yield and anisotropy, excited state lifetimes as well as energy transfer experiments give evidence for the occurrence of different enantiospecific binding modes. The photophysical properties of (*S*)-TFAE in the presence of polynucleotides are indicative of an intercalative binding mode with a clear dependence on the adenine–thymine (A–T) content of the DNA. Furthermore, the fluorescence quenching of (*S*)-TFAE in the vicinity of A–T pairs correlated with an increase of the fluorescence lifetime suggests that there are at least two different intercalative binding sites for this enantiomer. In contrast, (*R*)-TFAE does not recognize the synthetic polynucleotide poly-(dA-dT)-(dA-dT) and binds only by surface interactions with the natural DNA. Neither TFAE enantiomer binds to poly(dG-dC)-poly(dG-dC). This chiral discrimination for intercalative and base specific binding modes is explained in terms of the helical asymmetry and interactions with the A–T bases which is matched by the asymmetry of the *S* enantiomer but precludes intercalation by the *R* enantiomer.

The photophysical properties of TFAE have never been previously studied. The fluorescence quantum yield of the chromophore in cyclohexane and water was found to be 0.35 ± 0.04. The triplet state of free TFAE was characterized by its absorption spectrum (ε_{max} = 56000 M^{-1} cm^{-1} at 425 nm) and its formation quantum yield (φ_T = 0.7 ± 0.1). Biphotonic ionization occurred upon laser excitation of TFAE in water and the solvated electron and the radical cation were identified [ε ($TFAE^{\bullet +}$) = 8000 M^{-1} cm^{-1} at 720 nm]. The triplet and radical cation formation and decay kinetics of free TFAE were not altered by the presence of polynucleotides under the experimental conditions used.

Introduction

Chirality is a common property of biological molecules which plays a fundamental role in the recognition processes that occur naturally between them (protein–DNA interaction, enzymatic catalysis, antibodies activity, *etc.*). An interesting and challenging problem is the delineation of the molecular mechanisms involved in these specific interactions. One method of approach to this problem is to design molecules which interact enantiospecifically with their biological targets.[1–4] In this research area, chiral DNA binding agents have raised considerable interest as nano-probes of the nucleic acid sequence and topology. This research also offers considerable potential in the rational design of novel drugs and/or in the development of tools for biotechnology (DNA sequencing, antigen strategy, *etc.*).

Chiral inorganic compounds with transition metals have been shown to be highly specific chemical probes able to perform molecular recognition of the polymorphism of DNA, *i.e.* right-handed B DNA *vs.* left-handed Z DNA.[1] On the other hand, these chromophores have been shown to interact enantioselectively with DNA base sequences[2,3] just like other polycyclic aromatic compounds such as viologen derivatives.[4]

Pirkle's acid (2,2,2-trifluoro-1-(9-anthryl)ethanol; TFAE) is a chiral anthracene derivative. Its chirality is due to the presence of an asymmetric carbon atom in the trifluoroethanol group (Scheme 1). TFAE and its analogs have been extensively used for the enantioselective separation of drugs and amino acids using NMR spectroscopy and chromatographic methods;[5,6] however, they have never been tested as DNA sequence and/or topology probes. The planar aromatic polycyclic core of TFAE, comparable to the nucleic acid bases, suggests the possibility of intercalation of the chromophore into the double helix which may result in chiral recognition ability.

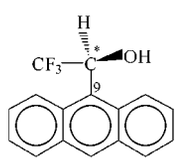

Scheme 1 Structure of (*S*)-2,2,2-trifluoro-1-(9-anthryl)ethanol [(*S*)-TFAE].

In order to check this possibility we have studied the binding of TFAE to DNAs of different purine–pyrimidine contents: the synthetic polynucleotides poly(dA-dT)-poly(dA-dT) and poly(dG-dC)-poly(dG-dC) and the natural calf thymus DNA (CT-DNA). Considering that TFAE is an optical sensor, its molecular interaction with nucleic acids was investigated using both steady state and time resolved spectroscopic methods. Different binding modes can thus be revealed, such as intercalation and surface binding (electrostatic interactions,

* Tel: 01 69 15 73 64, Fax: 01 69 15 67 77. E-mail: marie-pierre.fontaine-aupart@ppm.u-psud.fr

hydrogen bonds, *etc.*). Indeed, the formation of such complexes results in an ordered arrangement of the chromophore between the adjacent base pairs or in the DNA grooves, resulting in an electronic interaction and stabilization of the complexed molecule with the nucleic acids (*e.g.* π–π interactions, dipole–dipole). Such binding modes are expected to lead to substantial perturbations in the photophysical properties of TFAE: effects on the absorption spectra as well as on the fluorescence properties (quantum yields, anisotropy of the emission and fluorescence lifetimes, energy transfer). These spectroscopic measurements constitute an essential step of testing molecular recognition of the DNA structure by the chiral probe.

Another line of study consists of using the photosensitizing properties of the chromophore to discriminate between different diastereoisomers in the excited state.[7–10] Usually, such photochemical processes imply energy or electron transfer between the sensitizer (chromophore) and the acceptor (DNA) with a reaction rate dependent on the complex geometry, thus allowing enantiomeric discrimination. These photodynamic reactions that occur frequently in the excited singlet and/or triplet states of the chromophore as well as in its radical forms can be studied by absorption and fluorescence time resolved spectroscopy.

In this paper, we present a detailed steady state and time resolved spectral analysis of the fundamental and excited states (singlet and triplet) of TFAE–DNA complexes and of the radical cation of the chromophore obtained by biphotonic ionization. We provide evidence for different enantiospecific modes of binding of TFAE to DNA revealing this chromophore as a promising new nucleic acid molecular probe. A prerequisite for this investigation was the detailed study of the photophysical properties of free TFAE in solution which is reported here for the first time.

Experimental

Chemicals

(*R*)- and (*S*)-TFAE were obtained from Sigma and used as received. Typically, isomeric purity was 99.5% for each enantiomer. Cyclohexane and ethanol were of spectroscopic grade and KH_2PO_4, K_2HPO_4, NaCl, HCl of the highest grade available from Merck. In aqueous media, TFAE was first dissolved in HCl solution (Prolabo, Normapur) and then diluted in phosphate buffer prepared from twice distilled deionized water. The samples were deaerated by bubbling argon through the solution prior to the experiments. When necessary, the solvated electron was eliminated by saturation of the solution with N_2O and 0.05 M *tert*-butyl alcohol which scavenged the free $OH^{\bullet}$ radicals formed during the electron N_2O reaction. The oxygenated samples were obtained by maintaining 1 atm O_2 upon the solution. All the gases were from Alphagaz with a purity of 99.99%.

Calf thymus DNA and synthetic polynucleotides (average lengths > 500 base pairs) were purchased from Pharmacia and used as received without further purification. Purity of the polynucleotides and of DNA was checked by monitoring their circular dichroism (using a Jobin–Yvon Mark V automatic recording dichrograph) to ascertain the absence of a CD band below 240 nm. All samples were dissolved in 50 mM phosphate buffer (50 mM KH_2PO_4 and 50 mM K_2HPO_4) pH 7.0 containing 100 mM NaCl (buffer A). DNA concentrations per nucleotide were determined spectrophotometrically using the following molar absorption coefficients: $\varepsilon_{260\ nm} = 6600\ M^{-1}\ cm^{-1}$ for poly(dA-dT)-poly(dA-dT),[11] $\varepsilon_{254\ nm} = 8400\ M^{-1}\ cm^{-1}$ for poly(dG-dC)-poly(dG-dC),[12] $\varepsilon_{260\ nm} = 6600\ M^{-1}\ cm^{-1}$ for CT-DNA.[13]

Absorption measurements

Ground state absorption spectra were recorded at 25 °C using a PC-controlled Cary 210 (Varian) spectrophotometer using a 1 cm quartz cell. The concentration of TFAE was determined by weighing and used to estimate the molar absorption coefficient of the chromophore. The absorption titrations were performed by keeping the concentration of the chromophore constant while varying the nucleic acid concentration. This was done by adding an appropriate amount of DNA stock solution to an initial volume of TFAE in buffer (2 ml). The dilution effects were taken into account in order to maintain the TFAE concentration constant. The ratio of TFAE to polynucleotides ($1/r$) used in these experiments was varied from 0–40 step by step (16 points).

Transient absorption measurements were obtained using laser photolysis equipment described previously.[14] Briefly, the excitation source was a YAG laser (Quantel, YG 441) of 3 ns full width at half maximum with third harmonic (355 nm) generation. The 355 nm beam was directed onto one side of a 10 mm square silica cell containing the sample. The transient transmission variations were monitored at right angles to the excitation in a cross beam arrangement using a xenon flash lamp, a monochromator, a photomultiplier and a digitized oscilloscope interfaced with a microcomputer. Variations in the laser output were measured using a joulemeter receiving a small fraction of the laser light. The fluence of the incident laser pulse in the sample was obtained by calibration of the joulemeter using anthracene in deaerated cyclohexane (6.5×10^{-5} M) as a triplet actinometer.[15] The latter was also used to determine by the comparative method, the quantum yield Φ_T of singlet–triplet intersystem crossing for 355 nm excitation [eqn. (1)],

$$\Phi_T = \Phi_{T\ (anthracene)} \times [(A_t/E)^{TFAE}/(A_t/E)^{anthracene}] \times [\varepsilon_T{}^{anthracene}/\varepsilon_T{}^{TFAE}] \times [A_{/S}{}^{anthracene}/A_{/S}{}^{TFAE}] \quad (1)$$

where $A_t{}^{anthracene}$ and $A_t{}^{TFAE}$ were the maximum absorbances for anthracene and TFAE triplet absorption respectively, $E^{anthracene}$ and E^{TFAE} the excitation fluences, $\varepsilon_T{}^{anthracene}$ and $\varepsilon_T{}^{TFAE}$ the triplet molar extinction coefficients and $A_{/S}{}^{anthracene}$ and $A_{/S}{}^{TFAE}$ the absorbances of the ground state at the laser excitation wavelength. This method of determining quantum yields is valid if only a small fraction of the molecules are excited so that the absorbance obtained remains linear with the laser energy; in these measurements less than 10% of the TFAE and anthracene molecules were converted into the triplet state. Furthermore, the anthracene concentration was chosen to give the same absorbance at 355 nm as that of TFAE. The triplet concentration of anthracene was monitored at its absorption maximum (422 nm) using a triplet extinction coefficient of $6.47 \times 10^4\ M^{-1}\ cm^{-1}$ and a triplet quantum yield value of 0.71.[15]

Fluorescence measurements

Corrected steady state emission spectra were measured with a Perkin-Elmer MPF-3L spectrofluorimeter (3 nm slits in both excitation and observation monochromators) at 20 °C along a 1 cm optical pathlength. The emission spectrum of free TFAE was measured using 366 nm excitation and the spectra of TFAE–polynucleotides or DNA mixtures using 366 nm excitation or a wavelength between 290–296 nm for energy transfer experiments. At these excitation wavelengths, the absorbances were less than 0.1 making inner filter effects negligible.

The determination of the fluorescence quantum yields was carried out using anthracene in cyclohexane as a reference ($\lambda_{exc} = 366$ nm; $\Phi_f = 0.29$ in aerated conditions).[16] The fluorescence quantum yields Φ_f were calculated using the relationship in eqn. (2), where the subscript x refers to the unknown

$$\Phi_{fx} = \Phi_{f\ s}\, F_s A_x / F_x A_s \quad (2)$$

and the subscript s to the standard, A is the absorbance at the

Table 1 Fluorescence decay parameters of each enantiomer of TFAE in buffer A and complexed to the different polynucleotides

	τ_1/ns (±0.2 ns)	A_1 (±1%)	f_1 (%)	τ_2/ns (±0.5 ns)	A_2 (±1%)	f_2 (%)	$\langle\tau\rangle$ (±0.3 ns)	χ^2
(*R*)-TFAE	7.2	100	100	—	—	—	—	1.13
(*S*)-TFAE	7.1	100	100	—	—	—	—	1.2
(*R*)-TFAE–[poly(dA-dT)]$_2$	7.1	98	95	19.8	2	5	7.3	1.02
(*S*)-TFAE–[poly(dA-dT)]$_2$	7.2	94	86	19.8	6	14	7.9	1.02
(*R*)-TFAE–DNA	6.9	99	98	17	1	2.0	7.0	1.01
(*S*)-TFAE–DNA	6.9	99	98	19.1	1	2.0	7.0	1.14
(*R*)-TFAE–[poly(dG-dC)]$_2$	7.2	100	100	—	—	—	—	1.11
(*S*)-TFAE–[poly(dG-dC)]$_2$	7.2	100	100	—	—	—	—	1.12

excitation wavelength and F is the integrated emission across the band. The fluorescence titrations were performed as described above. However, in this case, a maximum value of $1/r \sim 80$ could be obtained.

Steady state anisotropy measurements were made on an SLM 4600 spectrophotometer employing Glan–Thompson calcite prism polarizers arranged in a "T" shaped geometry. Samples were excited at 366 nm and the emission was monitored by employing Corning glass filters. The orientation of the polarizers was checked by glycogen solutions. Several readings were averaged for a single measurement and the deviation was usually less than 5%. For these experiments, the ratio of TFAE to DNA ($1/r$) was kept to 1/20 to ensure maximum binding of the probe.

Time resolved fluorescence measurements were performed by the time correlated single photon counting method,[17] using synchrotron radiation as a source of the excitation light. The instrument used on the SA1 beam line of Super-ACO (LURE) has been previously described.[18] The width of the excitation pulse was routinely 650 ps FWHM, with a repetition frequency of 8.323 MHz.

The total fluorescence decays and fluorescence anisotropy decays were recorded as in ref. 18. The excitation was set at 366 nm ($\Delta\lambda = 9$ nm) and the emission was observed at 425 nm ($\Delta\lambda = 9$ nm). The instrumental function, $g(t)$ was recorded with a scattering solution of Ludox (DuPont Co.) at the emission wavelength, alternately with the parallel and the perpendicular components of the fluorescence [$I_{VV}(t)$ and $I_{VH}(t)$, respectively]. The correction factor, β, for the differing sensitivity to polarization was determined on free TFAE as in ref. 18. For each sample, approximately 8 million counts (giving approximately 4×10^4 counts in the peak channel) were stored in the total fluorescence decay [$I_{VV}(t) + 2I_{VH}(t)$] with each polarized curve being collected over 2048 channels at 49 ps per channel.

The different parameters given in Table 1 were extracted from the fluorescence decays after analysis by the maximum entropy method (FAME, MEDC Ltd, UK) as described previously,[19] except that 120 iterations were systematically performed. The resulting lifetime distribution $a(\tau)$ of pre-exponential factors *vs.* lifetime is split in as many species as well separated peaks. The lifetime τ_i and relative amplitude A_i of each species i are then defined by eqns. (3) and (4).

$$\tau_i = \frac{\int_{\text{peak}i} \tau a(\tau)\partial\tau}{\int_{\text{peak}i} a(\tau)\partial\tau} \quad (3)$$

$$A_i = \frac{\int_{\text{peak}i} a(\tau)\partial\tau}{\int_0^\infty a(\tau)\partial\tau} \quad (4)$$

The first order average fluorescence lifetime $\langle\tau\rangle$ is obtained from the lifetime distribution $a(\tau)$ according to eqn. (5). The

$$\langle\tau\rangle = \frac{\int_0^\infty \tau a(\tau)\partial\tau}{\int_0^\infty a(\tau)\partial\tau} \quad (5)$$

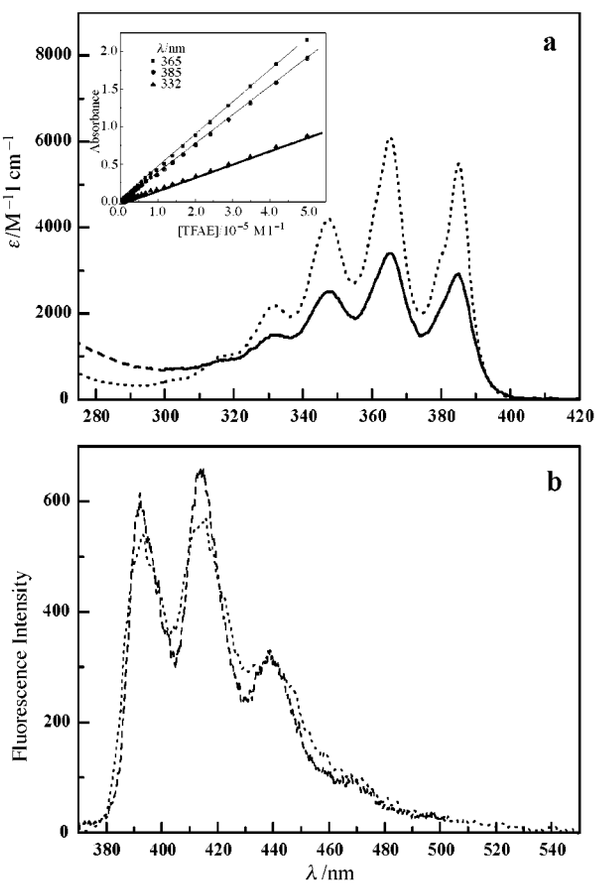

Fig. 1 a: Absorption spectrum associated to the first electronic transition of TFAE in cyclohexane (dashed line) and in buffer A (solid line). Inset: Verification of the Beer–Lambert law in buffer aqueous solution. b: Normalized fluorescence spectra (excitation wavelength 366 nm) of 3.7×10^{-5} M (*S*)-TFAE in cyclohexane (dashed line) and in buffer A (solid line).

fractional contribution of species i to the total fluorescence intensity is then: $f_i = A_i\tau_i/\langle\tau\rangle$. Error bars on individual lifetimes τ_i are based on the average width of the corresponding peak in the lifetime distribution. Error bars on the average lifetimes $\langle\tau\rangle$ are based on estimates of the repeatability of the measurements.

Results

Absorption properties of TFAE

The ground state absorption spectrum of TFAE was first measured in cyclohexane (Fig. 1a). As for anthracene, the lower energy absorption band corresponding to the $S_0 \rightarrow S_1$ transition, is characterized by a clear-cut vibrational progression with five peaks. However, these peaks are red shifted by 10 nm as compared to anthracene in cyclohexane and located at 385, 366, 349, 334 and 318 nm. Furthermore, broadening and hypochromicity of the absorption spectrum are observed ($\varepsilon_{\text{max}} =$

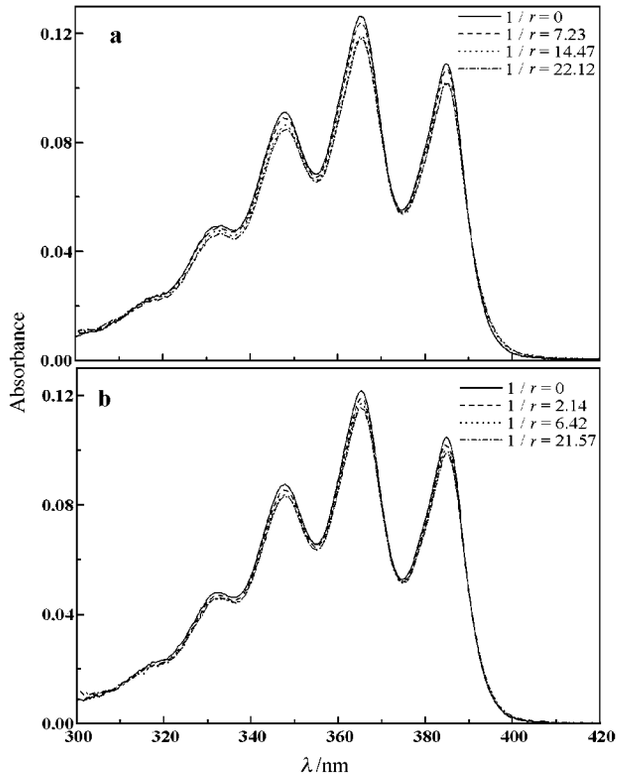

Fig. 2 Absorption spectra of (*S*)-TFAE in the presence of increasing amounts of poly(dA-dT)-poly(dA-dT) (part a) and CT-DNA (part b). For the sake of clarity, the data are only reported for four values of 1/*r*. [(*S*)-TFAE] = 3.7×10^{-5} M in buffer A.

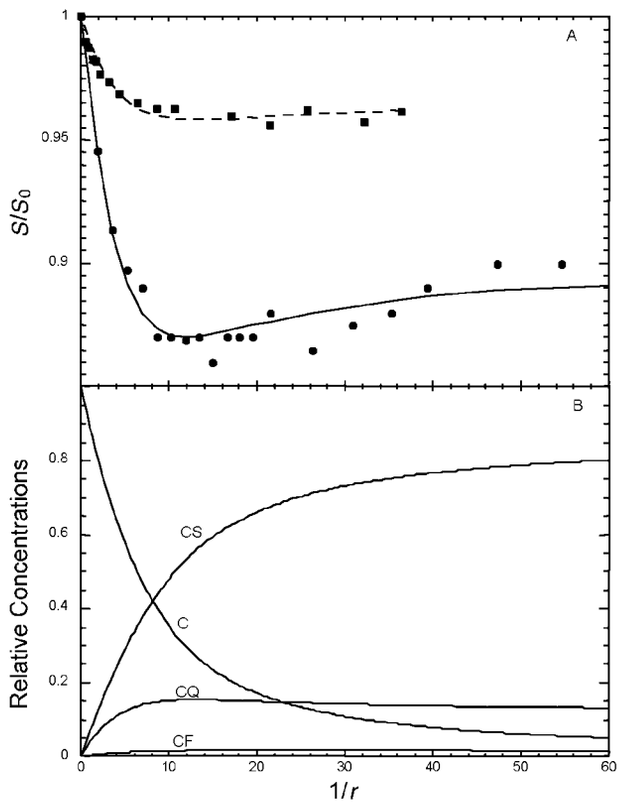

Fig. 3 A: Absorption (■) and fluorescence (●) titration curves of (*S*)-TFAE with poly(dA-dT)-poly(dA-dT). The dashed lines represent the best fitting of the experimental data. S/S_0 corresponds, for the absorption titration curve, to the ratio of the absorbance at the maximum wavelength 366 nm of the complex to that of the free chromophore for each 1/*r* value. The fluorescence titration curve corresponds to the ratio of the fluorescence quantum yield of the complex to that of the free chromophore. B: Evolution of the concentrations of free TFAE [C], non specific surface [CS], fluorescent intercalative [CF] and non fluorescent intercalative [CQ] complexes.

6500 M^{-1} cm^{-1} at 365 nm for TFAE compared to $\varepsilon_{max} = 9500$ M^{-1} cm^{-1} at 375 nm for anthracene). These results can be interpreted by the free rotation of the alkyl chain around the C*–C[9] bond resulting in an increase of the low frequency vibration mode density.

In aqueous solution the TFAE absorption spectrum is characterized by a significant decrease of the molar absorption coefficient ($\varepsilon_{365} = 3400$ M^{-1} cm^{-1}) compared to the spectrum in cyclohexane (Fig. 1a). This effect could be due to the low solubility of TFAE. Indeed, anthracene and its derivatives are known to be sparingly soluble in water.[20] However, we have checked the Beer–Lambert law for TFAE concentrations between 5×10^{-7} to 5×10^{-5} M (Fig. 1a, inset). Hence, we assume that over the concentration range used in this study the molecules in their ground state are solubilized and only exist as monomers. This higher solubility in water compared to anthracene can be explained by the polarity of the alkyl substituent. The adjunction of a polar group on the anthracene ring is commonly used to increase the solubility of the chromophore in aqueous solution.[21,22] Due to this TFAE polarity, the decrease of the molar absorption coefficient (with constant oscillator strength) can be explained by interactions between the chromophore and the solvent leading to a less resolved structure of the absorption spectra as already reported for similar anthracene derivatives.[22]

Absorption titration of TFAE with nucleic acids

Classical absorption titration experiments were used to assay binding of TFAE to the polynucleotides. Fig. 2 shows the changes in the electronic absorption spectra induced by adding increasing amounts of poly(dA-dT)-poly(dA-dT) (Fig. 2a) and CT-DNA (Fig. 2b) to a solution of (*S*)-TFAE. By increasing the nucleic acid concentrations different features can be distinguished depending on the DNA sequence. The absorption spectra of (*S*)-TFAE in the presence of increasing amounts of poly(dA-dT)-poly(dA-dT) from zero up to $1/r \sim 20$ were characterized by a hypochromic effect (~10% at 365 nm) and the presence of an isosbestic point at 390 nm (Fig. 2a) which support the formation of a (*S*)-TFAE–polynucleotide complex in the ground state. Fig. 3A shows that this hypochromic phase is followed, for 1/*r* higher than 20, by a slight absorption increase, suggesting the possible occurrence of another binding mode (see below). The extent of hypochromism was found to be smaller in the presence of CT-DNA (3%) but the isosbestic point was still present (390 nm). In contrast, in the presence of poly(dG-dC)-poly(dG-dC), from the free chromophore up to a ratio of polynucleotides to TFAE $1/r \sim 40$, no change in the absorption spectra is observed.

No absorption spectral changes were observed when (*R*)-TFAE was in the presence of any of these different polynucleotides. The absorption spectral changes observed for each enantiomer of TFAE in the presence of nucleic acids provide a first specific measure of stereoselectivity for TFAE binding to nucleic acids.

Steady state fluorescence properties of TFAE

Corrected fluorescence emission spectra of TFAE in cyclohexane and buffer solution are represented in Fig. 1b. In each case, the emission spectrum is the mirror image of the absorption spectrum. There is a vibrational progression based on a 1350 cm^{-1} mode with three distinct maxima located at 395 nm, 415 nm and 439 nm. The shape of the emission spectrum of TFAE is very similar whatever the solvent, only a slight broadening is observed in aqueous solution.

The fluorescence quantum yields of TFAE also have nearly the same value in all solvents ($\Phi_f = 0.35 \pm 0.04$), similar to that

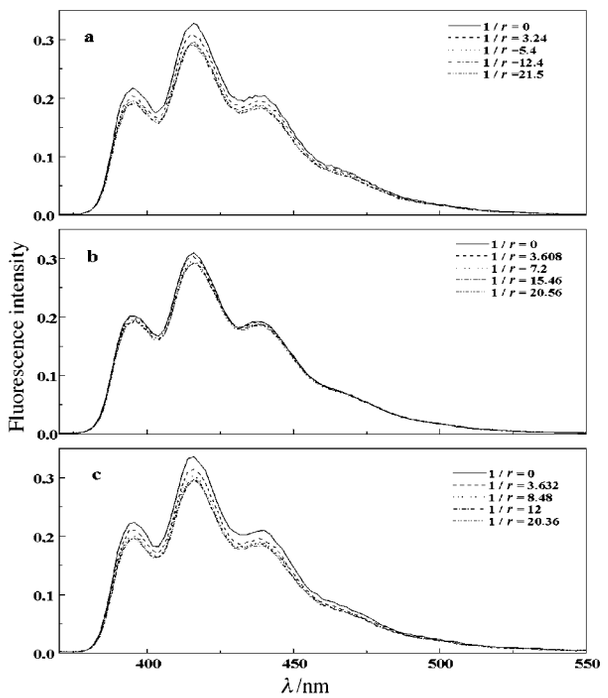

Fig. 4 Fluorescence spectra of (*S*)-TFAE with increasing concentration of poly(dA-dT)-poly(dA-dT) (part a) and CT-DNA (part b) upon excitation at 366 nm in buffer A. For the sake of clarity, the spectra corresponding to $1/r > 20$ associated with an increase in fluorescence (Fig. 3A) are not represented. c: Fluorescence spectra of (*R*)-TFAE–CT-DNA complexes for $1/r$ varying from 0–20 under identical experimental conditions as used for (*S*)-TFAE.

of anthracene in cyclohexane.[16] The radiative lifetime was determined from this quantum yield value and that of the fluorescence lifetime ($\tau_f = 7$ ns in buffer solution, see below) according to eqn. (6). A value of 20 ns was obtained, signifi-

$$\tau_R = \tau_f/\Phi_f \qquad (6)$$

cantly higher than the radiative data for anthracene (13 ns calculated from the data in ref. 16). This result indicates that the S_0–S_1 transition is less allowed for TFAE than for anthracene, which is consistent with the different absorption intensities measured for the two chromophores.

Fluorescence emission of TFAE complexed with nucleic acids

The changes in fluorescence spectrum induced upon binding of TFAE to various amounts of poly(dA-dT)-poly(dA-dT) and CT-DNA together with the fluorescence spectrum of free TFAE are shown in Fig. 4. As observed for the absorption measurements, the emission spectra of both TFAE enantiomers do not change in shape or intensity in the presence of poly(dG-dC)-poly(dG-dC) for $1/r$ varying from 0 to 80. Binding of (*S*)-TFAE to poly(dA-dT)-poly(dA-dT) (Fig. 4a) and CT-DNA (Fig. 4b) was found to quench the probe fluorescence without spectral change to a maximum extent of 12% and 4% respectively.

The maximum quenching effect is observed for $1/r \sim 20$ and as previously reported for absorption titration (Fig. 3A), the fluorescence increases significantly for $1/r$ from 20 up to 80, suggesting again different distributions of the chromophore on the polynucleotide.

The fluorescence spectra of (*R*)-TFAE do not change upon complexation with poly(dA-dT)-poly(dA-dT), but a significant quenching of the emission (15%) is observed for (*R*)-TFAE–CT-DNA complexes (Fig. 4c) despite no detectable effect on absorption titration.

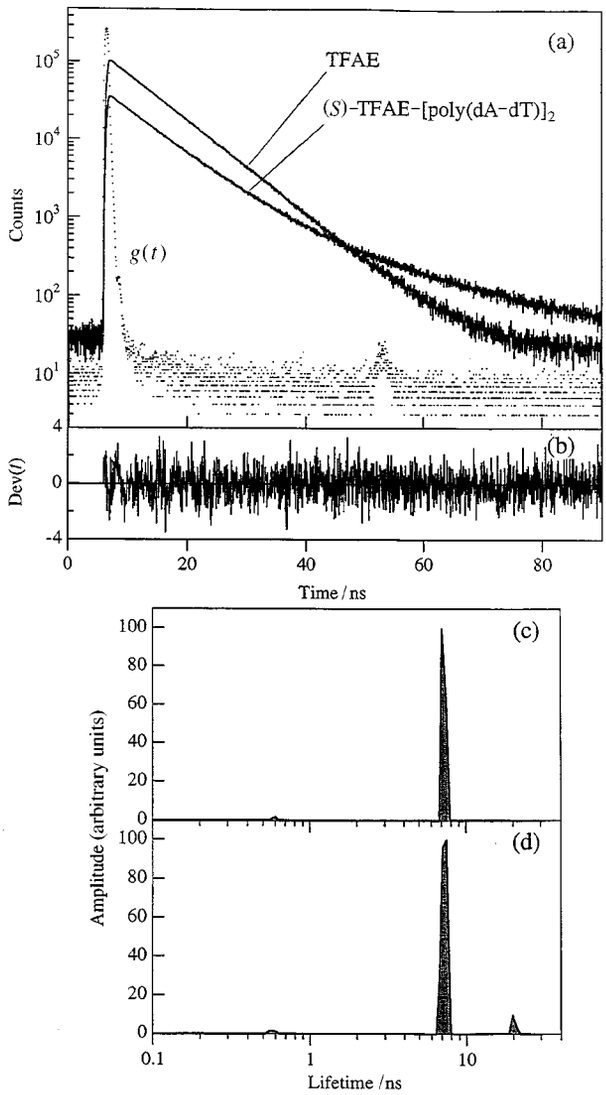

Fig. 5 Time resolved fluorescence of TFAE in the absence and presence of poly(dA-dT)-poly(dA-dT). Experimental data: (a) instrumental function $g(t)$ and total fluorescence decays reconstructed from $I_{VV}(t)+2\beta I_{VH}(t)$; (b) fitting residuals of model to the (*S*)-TFAE–poly(dA-dT)-poly(dA-dT) data; (c) and (d) fluorescence lifetime distributions recovered for free TFAE and (*S*)-TFAE–poly(dA-dT)-poly(dA-dT) respectively. Experimental conditions as in Fig. 4.

Time resolved fluorescence studies

As observed from the steady state fluorescence results, the fluorescence dynamic parameters for each TFAE enantiomer appear sensitive to the nature of the DNA sequence. The fluorescence decay profile of (*S*)-TFAE shows a distinct biexponential behavior in the presence of poly(dA-dT)-poly(dA-dT) (Fig. 5a). Deconvolution of the decay traces using the maximum entropy method resulted in a short lived component of 7 ns, the same as that measured for TFAE in the absence of polynucleotide (Fig. 5c) and a long lived component of 20 ns but with a low amplitude (Fig. 5d, Table 1). For the (*R*)-TFAE in the presence of poly(dA-dT)-poly(dA-dT), a similar long lived, small amplitude component was also detected due to the sensitivities of the measurement and the analysis (Table 1), but cannot be interpreted at this time.

In the presence of CT-DNA, the fluorescence decay of each TFAE enantiomer is characterized essentially by a nearly single emission lifetime of 7 ns (Table 1). The preexponential factor (A) of the long lived component is less than 1% corresponding to a signal contribution of ~2% (Table 1). This value can not be taken as meaningful since it could be greatly affected even by a small change in the long lived fluorescence lifetime. As observed

Table 2 Steady state fluorescence anisotropy for TFAE in the presence of polynucleotides. For each complex, $1/r = 20$ and [TFAE] = 40 μM in buffer A, at pH 7.0. The fluorescence anisotropy for each TFAE enantiomer in buffer A is zero

	TFAE–DNA		TFAE–poly(dA-dT)-poly(dA-dT)		TFAE–poly(dG-dC)-poly(dG-dC)	
	R	*S*	*R*	*S*	*R*	*S*
Anisotropy	6.6×10^{-4}	4.6×10^{-3}	6.66×10^{-4}	6.68×10^{-3}	0.00	6.66×10^{-4}

in the steady state measurements, the dynamic fluorescence properties of each enantiomer are not changed in presence of poly(dG-dC)-poly(dG-dC).

Fluorescence anisotropy measurements

The binding mode of a chromophore to DNA may be distinguished by steady state and time resolved emission anisotropy experiments. When a chromophore intercalates into the helix or in a DNA groove, its rotational motion should be restricted since it is rigidly held with long residence times on the timescale of the emission lifetime. Thus, the fluorescence from this bound chromophore should be more polarized than that of the free compound.

The stationary anisotropy results are summarized in Table 2. In the absence of DNA, fluorescence of the TFAE chromophore was not polarized due to the rapid tumbling motion of the compound in aqueous medium. On the other hand, we did not observe any anisotropy of the emission for each TFAE enantiomer with poly(dG-dC)-poly(dG-dC) as well as for (*R*)-TFAE with the different double helix biopolymers investigated. However when (*S*)-TFAE binds to DNA containing alternating A–T sequences, the fluorescence is significantly polarized, suggesting again a strong interaction of this enantiomer with the polynucleotide. Similarly, significant anisotropy was obtained for (*S*)-TFAE with CT-DNA with a value consistent with the A–T base pairs probability. These anisotropy values are consistent with the results obtained for several DNA intercalated chromophores.[22,23] They appear relatively weak compared to the limiting value in a rigid medium (~0.4) and reflect the low extent of the nucleic acid–TFAE association and/or the flexibility of the double helix–chromophore complex.

The fluorescence anisotropy decays were measured for free TFAE and TFAE–poly(dA-dT)-poly(dA-dT), the only complex for which the fluorescence properties are significantly different from those measured for the chromophore in solution. The very fast anisotropy decay of free TFAE (Fig. 6a) being at the limit of our time resolution, the exact rotational correlation time of the free probe cannot be recovered from the data but is estimated to be a few hundred picoseconds (with a high residual chi-square of 1.44). The fluorescence anisotropy decay of the (*S*)-TFAE–poly(dA-dT)-poly(dA-dT) complex clearly shows a biphasic behavior (Fig. 6b) characterized by a first rapid decay similar to that of the free probe, followed by a slow increase. In this case, the multiexponential analytical model used in our current method of data analysis is clearly inapplicable and therefore no curve fitting results will be presented. This situation is typical of systems where a specific association exists between, on the one hand, a short fluorescence lifetime component with rapid rotational dynamics and on the other hand, a long fluorescence lifetime with slow rotational dynamics.[24]

Fluorescence sensitization by DNA bases

The singlet–singlet energy transfer from the nucleic acid bases to the TFAE chromophore was probed by monitoring the TFAE fluorescence spectrum obtained upon excitation into the DNA absorption bands (λ_{exc} between 290–296 nm, a spectral range where ~90% of light was absorbed by nucleic acid bases). The emission spectra of both TFAE enantiomers in the presence of poly(dG-dC)-poly(dG-dC) and of (*R*)-TFAE in the presence of poly(dA-dT)-poly(dA-dT) and CT-DNA were identical to those of the free chromophores in solution. In contrast, excitation at 292 nm of the (*S*)-TFAE–poly(dA-dT)-poly(dA-dT) complex resulted in a significant increase of the fluorescence (50%) (Fig. 7a), associated with a spectral deformation and broadening of the emission band. A similar but less intense result was also obtained for the (*S*)-TFAE–CT-DNA complex (Fig. 7b).

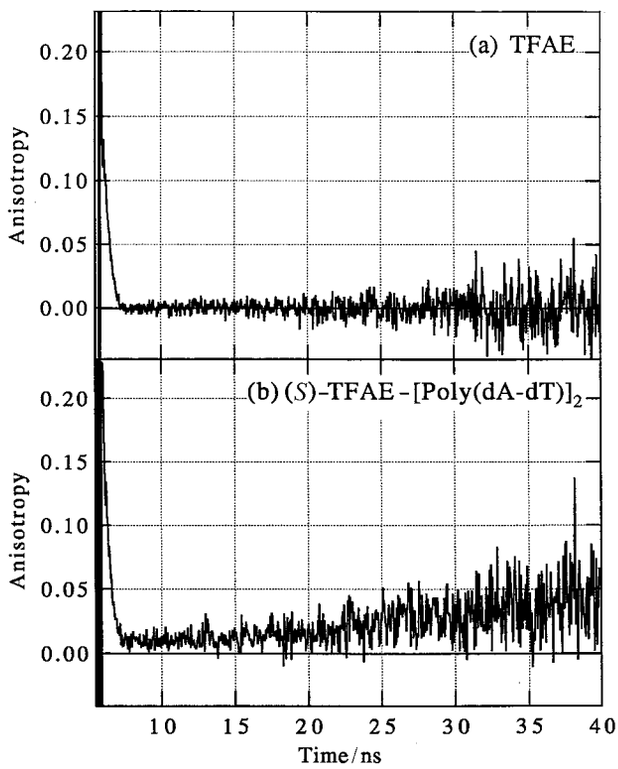

Fig. 6 Experimental, undeconvoluted fluorescence anisotropy decays $I_{VV}(t) - \beta I_{VH}(t)/[I_{VV}(t) + 2\beta I_{VH}(t)]$ of (a) free TFAE and (b) (*S*)-TFAE–poly(dA-dT)-poly(dA-dT) under experimental conditions as in Fig. 4.

This observation clearly establishes energy transfer from the singlet excited state of the nucleic acid bases to the excited singlet state of the (*S*)-TFAE chromophore, a result in agreement with the spectral overlap between DNA emission and TFAE absorption. This energy transfer is generally described using the Förster model, considering the spin-allowed character of the electronic transitions in the donor and the acceptor and the lack of accurate data on their relative distance and orientation. According to this model, the $1/R^6$ dependence of energy transfer (R is the distance between the species involved) as well as the very low quantum yield of the bases (10^{-5}–10^{-4}) (*i.e.* a very short excited state lifetime in the picosecond range[25]), implies sufficiently close proximity between DNA bases and the chromophore for this process to occur. This energy transfer process has been taken as a strong indication for an intercalating mode of binding.[26,27]

The Förster critical distance (R_0), for which 50% of the donor energy is transferred, may be calculated. The overlap integral was determined by eqn. (7), where $\varepsilon_A(\nu)$ is the molar

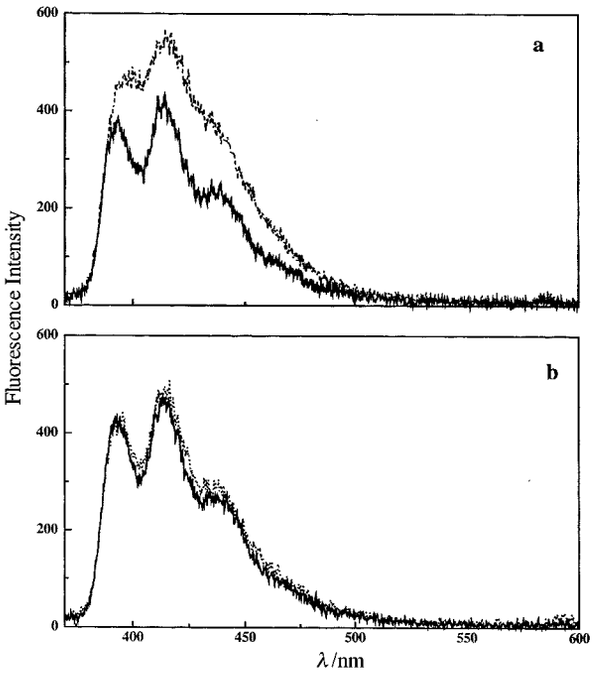

Fig. 7 Enhancement of (*S*)-TFAE emission, upon excitation at 292 nm, in the presence of different polynucleotides as a result of energy transfer ($1/r = 20$). a: Spectrum of the free chromophore (solid line) compared to the sensitized emission spectrum of (*S*)-TFAE in the presence of poly(dA-dT)-poly(dA-dT) (dashed line). b: Under the same conditions, the emission spectra of free (*S*)-TFAE (solid line) and (*S*)-TFAE–CT-DNA complex (dashed line).

$$J = \int_0^\infty \frac{F_D(\bar{\nu})\varepsilon_A(\bar{\nu})}{\bar{\nu}^4} d\bar{\nu} \sim 1.57 \times 10^{-15}\ M^{-1}\ cm^3 \qquad (7)$$

absorption coefficient of TFAE at the wavenumber ν and $F_D(\nu)$ is the fluorescence intensity of DNA at ν measured by Daniels.[28] The Förster critical distance is then given by eqn. (8),[29] where

$$R_0 = \sqrt[6]{\frac{9000 \ln 10 \Phi_D(\frac{2}{3})}{128\pi^5 n^4 N} J} \qquad (8)$$

n is the DNA refractive index ($n = 1.4$), N = Avogadro's number and the 2/3 fraction is the κ^2 value corresponding to an average over all possible relative orientations between the transition moments of the donor and the acceptor. Under the approximation that the emission spectra and the fluorescence quantum yields of the polynucleotide and DNA are the same ($\Phi_D = 2 \times 10^{-5}$),[28] the critical Förster distance is calculated to be $R_0 \sim 4$ Å. If TFAE is intercalated between two base pairs, then the distance between the chromophore and each base is <3.4 Å (distance between two base pairs). Therefore considering this R_0 value, an efficient energy transfer is expected from the proximal DNA bases.

Transient absorption measurements

In order to determine whether TFAE could induce specific reactions in the triplet excited state and/or as a radical species with the nucleotide bases, laser flash photolysis experiments have been carried out in the presence and absence of polynucleotides.

The 355 nm laser photolysis of argon flushed TFAE in buffer solution (pH 7), associated to a spectral analysis between 380–780 nm, allowed us to characterize the transient absorption of the chromophore (Fig. 8c). This absorption spectrum was identical for each enantiomer and presented two distinct bands, centered at 425 nm and 700 nm respectively.

Triplet absorption characterization of TFAE (^{3}TFAE). The absorption transition at 425 nm is quenched by oxygen (1 atm) with a rate constant of $1.6 \times 10^9\ s^{-1}$ suggesting that this transient could be attributed to a $T_1 \rightarrow T_n$ absorption band of TFAE. The linear dependence of the absorbance variations with the laser fluence (Fig. 8a), characteristic of a monophotonic process, is consistent with this assignment. The adjunction of an asymmetric carbon and a fluoro group on the anthracene chromophore does not affect its triplet characteristics as revealed by the similarity between the triplet spectra and kinetics of TFAE and anthracene.[30] Indeed, in deaerated solutions, the ^{3}TFAE lifetime was found to be ~20 μs, corresponding probably to the same prevailing triplet–triplet annihilation process as that observed for anthracene.

Triplet quantum yield determination. The triplet quantum yield (Φ_T) of TFAE was first measured in cyclohexane since no photoionization process occurred in this solvent (see below). Using the method described in the Experimental section, we obtained $\Phi_{T\ TFAE} \times \varepsilon_T^{TFAE} = 0.86\ \Phi_{T\ anthracene} \times \varepsilon_T^{anthracene}$ (Fig. 8a). The determination of the molar absorption coefficient of the TFAE triplet was undertaken by simulating complete conversion of the TFAE ground state to the triplet state (Fig. 8b). This was achieved by multiplying the experimental transient absorption measurements by an appropriate coefficient x. Different values of x were tried and thus the resulting absolute spectrum of the triplet was compared with that of the ground state of the molecule. Under the assumption that the triplet spectrum was different from that of the ground state between 320 and 400 nm, acceptable x values lay in the range 8–12. Under these conditions, the ε_T^{TFAE} maximum value at 425 nm was estimated to be $56000 \pm 20\%\ M^{-1}\ cm^{-1}$ (Fig. 8b), leading to a TFAE triplet quantum yield equal to 0.7 ± 0.1, a value consistent with the fluorescence quantum yield obtained in these solvent conditions ($\varphi_f = 0.35$, see above).

The triplet quantum yield determination was also undertaken in buffer solution. Under these conditions we obtained $\Phi_{T\ TFAE} \times \varepsilon_T^{TFAE} = 0.54\ \Phi_{T\ anthracene} \times \varepsilon_T^{anthracene}$ (Fig. 8a). Since, in water, the TFAE radical cation absorption spectrum was superimposed on the triplet spectrum, the determination of ε_T^{TFAE} as described previously was impossible. Considering that the fluorescence quantum yield was found to be the same in cyclohexane and water, it was assumed that the triplet quantum yield is also the same in both solvents. Under this assumption, a ε_T^{TFAE} value of $28000\ M^{-1}\ cm^{-1}$ was obtained at 425 nm for the TFAE triplet in water.

Photoionization of TFAE. The near infrared absorption (700 nm), also observed at the end of the laser pulse (Fig. 8c), is characteristic of the solvated electron ($e^{\bullet -}_s$) which has a maximum at 715 nm in water.[31] In agreement with this assignment, the decay rate of this band was strongly increased by N_2O or O_2 addition (see below). Furthermore, we observed a quadratic dependence of the absorbance changes at 700 nm on the laser fluence (data not shown), characteristic of a biphotonic process. This result revealed the occurrence of an electron photoejection from the excited TFAE to produce the radical cation $TFAE^{\bullet +}$.

The apparent photoionization yield was calculated from the absorbance changes at 700 nm at the end of the laser pulse in the presence of $e^{\bullet -}_s$ (deaerated solution) and in the absence of $e^{\bullet -}_s$ (solution saturated with N_2O) using the molar extinction coefficient of $e^{\bullet -}_s$ at this wavelength. It was found that ~20% (±2%) of TFAE was photoionized in aqueous solution.

In the spectral range where the TFAE triplet state does not absorb ($\lambda > 600$ nm), the absorption spectrum of the TFAE radical cation may be directly revealed on removal of the strongly absorbing $e^{\bullet -}_s$. The solution was saturated with N_2O which quenched $e^{\bullet -}_s$ with a rate constant of $8.7 \times 10^9\ M^{-1}\ s^{-1}$. The resulting spectrum measured after disappearance of $e^{\bullet -}_s$ (100 ns) presented a peak near 720 nm (Fig. 8c) consistent with

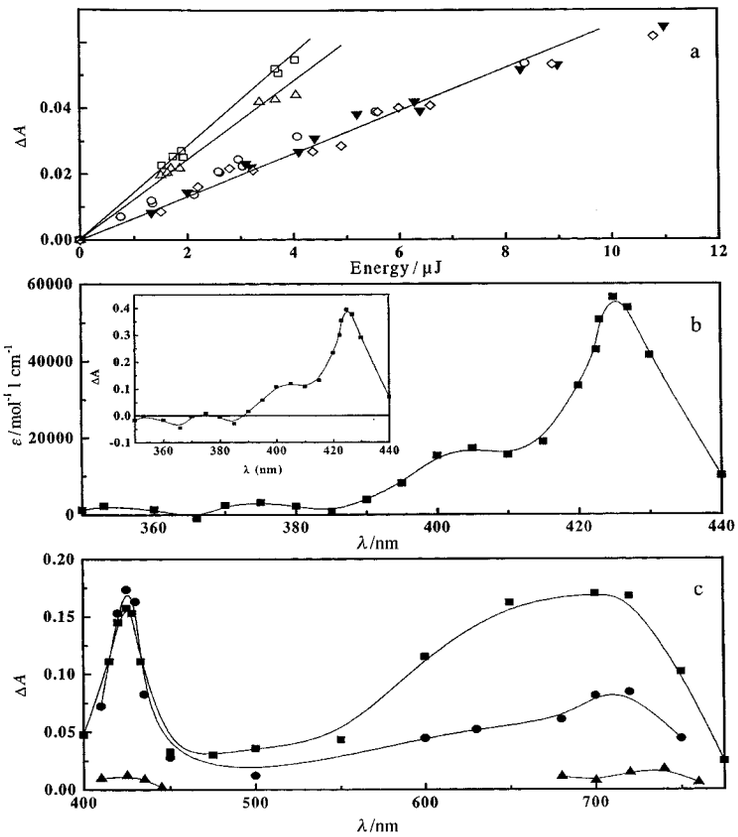

Fig. 8 a: Transient absorption at 422.5 nm due to the triplet population on laser excitation of 10^{-5} M anthracene in cyclohexane plotted against the laser energy (□), transient absorbance at 425 nm due to the triplet population of 3.7×10^{-5} M TFAE in cyclohexane (△), in buffer A (○) and in the presence of poly(dA-dT)-poly(dA-dT) [(▼) (*S*)-TFAE–poly(dA-dT)-poly(dA-dT); (◇) (*R*)-TFAE–poly(dA-dT)-poly(dA-dT)] ($1/r = 20$). b: Calculated absorption spectrum of TFAE triplet in cyclohexane (see text). Inset: differential end-of-pulse transient absorption spectrum measured upon excitation of 3.7×10^{-5} M TFAE in cyclohexane by a 355 nm laser pulse. c: Transient absorption spectra of TFAE in deaerated cyclohexane solution at the end of the laser pulse (■), in N_2O saturated solution, 100 ns after the end of the laser pulse (●) and in O_2 saturated solution, 40 μs after the end of the laser pulse (▲).

the anthracene radical cation spectrum previously observed by pulse laser and radiolysis experiments.[32] Considering the apparent photoionization quantum yield value, we estimated a maximum molar absorption coefficient for the $TFAE^{\bullet+}$ radical of 8000 M^{-1} cm^{-1}. The decay of this species occurred on the microsecond timescale with a lifetime of 15 μs.

In the presence of oxygen, we also observed a microsecond decay of the radical cation absorption. The rate of this process was identical under one oxygen atmosphere or atmospheric pressure, indicating that the radical does not react directly with O_2. A good fitting of the decay curve was obtained with second order kinetics ($k = 3.5 \times 10^9$ M^{-1} s^{-1}). Most probably, the radical cation reacts with the superoxide ion formed by the fast reaction of oxygen with the solvated electron. The residual absorption observed at the longer times (~40 μs) (Fig. 8c) may thus be assigned to the species generated by this reaction.

Transient absorption of TFAE in presence of nucleic acids. The spectro-dynamic evolution of TFAE in the presence of nucleic acids [poly(dA-dT)-poly(dA-dT), poly(dG-dC)-poly(dG-dC) and CT-DNA] after 355 nm laser excitation, is not very sensitive to the nucleic acid environment. Both the triplet state formation (Fig. 8a) and the biphotonic ionization process are still effective with the same quantum yields as those measured for the free chromophore. The decays of the transient species, whatever the enantiomer nature, also occur on the same timescale without spectral evolution. This was thought to be a consequence of the absence of intramolecular charge transfer between the nucleotides and the TFAE triplet state or radical cation but may be due also to a low extent of complexation of TFAE.

Discussion

The results of these varied experiments, when considered together, provide a picture of the factors controlling the specific interaction of each enantiomer of TFAE with the nucleic acids. An important finding is the dependence of the spectroscopic properties of the chromophore on the base sequence and the topology of DNA. Since the fluorescence results reveal a complex picture, it is relevant to consider first any evidence for the occurrence of different binding modes that the various spectroscopic techniques may provide.

Enantiomeric selectivity of binding

1 (*S*)-TFAE. *1a Evidence for different binding modes.* In the studies of the binding nature of a chromophore to DNA, the fundamental problem is to distinguish an intercalative binding mode between DNA base pairs from a groove binding of the helix or a non specific surface interaction. The occurrence of energy transfer from the bases of poly(dA-dT)-poly(dA-dT) and CT-DNA to the (*S*)-TFAE provides the strongest support by photophysical methods for an intercalative binding of the chromophore. According to the experimental results, the calculation of the Förster critical distance indicates that the photoexcited DNA bases cannot be more than ~4 Å away from bound TFAE in order to transfer 50% of their absorbed energy to the chromophore. Hence, substantial energy transfer can occur only if bound (*S*)-TFAE is located in close proximity to the bases and with an adequate orientation (the dipole emission and absorption moments of the donor and the acceptor must be respectively in parallel planes) as is the case for intercalation. A chromophore bound on the helix exterior or in the DNA

grooves would be too far away and/or poorly oriented with respect to the bases to allow efficient singlet–singlet energy transfer. Such energy transfer from the DNA bases has been typically observed with intercalating chromophores[33] particularly with anthracene derivatives.[34] The steady state absorption and fluorescence results, together with the results of time resolved fluorescence studies are consistent with strong binding of (*S*)-TFAE to DNA such as intercalation. Indeed, the addition of poly(dA-dT)-poly(dA-dT) or CT-DNA to a (*S*)-TFAE aqueous solution induces a hypochromism of the first absorption band of the chromophore simultaneously with the appearance of an isosbestic point which is typical of stacking interactions with the base pairs.[22,35,36] The polarization of the fluorescence of (*S*)-TFAE upon complexation with nucleic acids associated with slow rotational dynamics, indicating restrictive motions of the chromophore compared to the case of the free form is also consistent with an intercalative binding mode. The existence of a long lived fluorescence decay time ($\tau_f \sim$ 20 ns) also supports this assumption since it reflects a reduced efficiency of the non radiative deactivation pathway due to shielding of the chromophore from the aqueous solvent.

Taking into account the decrease of the fluorescence quantum yield of (*S*)-TFAE upon complexation with polynucleotides and the constancy of the triplet quantum yield, it must be concluded that the non radiative deactivation yield (dynamic and/or static processes) should increase upon complexation. There is no evidence in the time resolved fluorescence data for dynamic quenching which should be correlated to a decrease in the fluorescence lifetime. Therefore it is necessary to postulate that upon complexation with nucleic acids, the (*S*)-TFAE enantiomer when excited, can deactivate by fluorescing or *via* a non radiative pathway faster than the excited singlet state lifetime. Such a static fluorescence quenching has been commonly reported for a number of polycyclic planar molecules.[22,36,37] Often, this effect has been assigned to an electron transfer from the nucleic acid bases to the excited polycycle. The transient absorption measurements of (*S*)-TFAE–poly(dA-dT)-poly(dA-dT) did not show any evidence for any radical ion absorption, in particular that of the adenine radical cation characterized by a maximum around 630 nm. Such spectral changes may be too weak to be detected (see below). Alternatively, it is possible that the fast deactivation of the S_1 state of the chromophore is due to a non radiative $S_0 \leftarrow S_1$ transition *via* a low-lying and very short lived charge transfer state, a mechanism which has been proposed already for several intercalating molecules.[35,38]

Concerning the possible excited state interactions of intercalated (*S*)-TFAE and the neighboring DNA base pairs, the laser flash photolysis results suggest that no charge transfer processes occur between the triplet state or the radical cation of the chromophore and the nucleic acid bases. Furthermore, it is generally observed that the triplet excited state of an intercalating agent is protected from oxygen accessibility resulting in slower decay kinetics. This is not observed for (*S*)-TFAE intercalated in poly(dA-dT)-poly(dA-dT) and CT-DNA; it is thus concluded that the intercalated fraction of (*S*)-TFAE is too small to be detected in its excited states as predicted by our binding model (see below).

1b Binding constant. In an attempt to estimate the binding constants of the (*S*)-TFAE to poly(dA-dT)-poly(dA-dT), the absorption and fluorescence titration curves represented in Fig. 3A were analyzed. Using the fluorescence data (Table 1), we have tested a model involving the presence of free chromophores and both fluorescent and non fluorescent intercalated ones. In the hypothesis of non cooperative binding, the equilibrium constants can be written as $K_F = [CF]/([C][BF])$ and $K_Q = [CQ]/([C][BQ])$, where [C], [CF], [CQ], [BF] and [BQ] are respectively the concentrations of free chromophore, fluorescent complexed chromophore, non fluorescent complexed chromophore, free sites for fluorescent intercalated molecules and free sites for non fluorescent ones. In the titration experiments, we have a constant total chromophore concentration $[C]_0$, and a varying total site concentration $[B]_0$, with $r = [C]_0/[B]_0$.

Moreover, it is considered that the measured signal is proportional to the reactants concentrations. In consequence, the titration curves can be expressed as eqn. (9), where S/S_0 is the

$$S/S_0 = ([C] + \beta[CF] + \gamma[CQ])/[C]_0 \quad (9)$$

ratio of the absorbance or the fluorescence intensities of the complex to that of the free chromophore, β is the ratio between the observed property of the complex (maximum molar absorption coefficient or fluorescence quantum yield) and that of the unbound chromophore respectively for the fluorescent intercalated (*S*)-TFAE and γ is the corresponding ratio for the non fluorescent intercalated one (the absorption and fluorescence measurements have been performed in regions where the polynucleotide has only negligible absorption).

According to the experimental results, it was not possible with two such equilibrium models to fit both titration curves with physically acceptable parameters. It was therefore postulated that (*S*)-TFAE has also the possibility to bind to the polynucleotide by an additional mode. The equilibrium constant corresponding to the latter mode can be written as $K_B = [CS]/([C][BS])$, where [CS], [C] and [BS] are respectively the concentrations of bound chromophore, free chromophore and free sites for this additional binding mode. The titration curves can now be expressed as eqn. (10).

$$S/S_0 = ([C] + a[CS] + \beta[CF] + \gamma[CQ])/[C]_0 \quad (10)$$

The values of the equilibrium constants were obtained by simultaneous non linear χ^2 fitting of both titration curves (Fig. 3A). The best fit of the data gave intercalative binding constants for the fluorescent and non fluorescent intercalated forms of $8 \pm 5 \times 10^3\ M^{-1}$ and $8.7 \pm 0.7 \times 10^2\ M^{-1}$ respectively and a constant of $7.1 \pm 0.2 \times 10^4\ M^{-1}$ for the additional binding mode. Furthermore, for this latter mode, the values of a for both absorption and fluorescence signals are necessarily close to one, indicating that the photophysical properties of this complexed chromophore are not very different from those of the free one. The concentrations of the free chromophore and its complexes as a function of the base ratio are shown in Fig. 3B. The low extent of intercalation of (*S*)-TFAE did not allow an accurate determination of the β and γ parameters. However, the model suggests that the non fluorescent intercalating mode is associated with a hypochromicity of the absorption while the fluorescent intercalating one corresponds to an increase of both absorption and fluorescence intensities.

These results show that (*S*)-TFAE intercalates into the helix but to a lesser extent than expected for an anthracene chromophore.[22] This can be explained by considering the presence of the bulky CF_3 substituent twisted out of the anthracene plane leading to a partial insertion of TFAE and thus precluding substantial overlap with the base pairs. These low intercalation constants can also explain the absence of effect on transient absorption spectra and kinetics of the complex compared to the free chromophore as well as the low amplitude of the long lived fluorescence decay component (Table 1).

The additional binding mode of higher affinity for DNA than the intercalative ones may be a surface complexation due to the electrostatic interactions that usually occur with the charged surface of the double helix. Indeed, the presence of the strongly electron-attracting CF_3 group increases the acid character of both the hydrogen atom and the OH group on the asymmetric carbon, which polarizes the π electrons of the anthracene ring, conveying to TFAE the ability to form intermolecular interactions.[39]

2 (*R*)-TFAE. When (*R*)-TFAE was in the presence of poly-

nucleotides, we observed a significant fluorescence quenching only in the case of the (*R*)-TFAE–CT-DNA complex. Nevertheless, singlet–singlet energy transfer, fluorescence anisotropy or long lived fluorescent decay were not detected, thus excluding an intercalative binding mode of this enantiomer. Likewise, the absence of any effect on the absorption spectra reveals that there is no strong association between (*R*)-TFAE and CT-DNA in the ground state. Therefore, the fluorescence quenching can be explained by the formation of a specific complex (which gives rise to static quenching as described above) due to the interaction of (*R*)-TFAE with the DNA surface. Such a complexation could derive stereo-selectivity from association of the chiral chromophore with the asymmetric groove of the DNA depending on the helix topography. This fluorescence quenching only observed for the (*R*)-TFAE–CT-DNA complex provides a specific photophysical characterization of the interaction of the enantiomer with the DNA surface.

Binding localization

The photophysical properties of (*S*)-TFAE complexed to polynucleotides allow us to specify the chromophore localization inside the double helix. Indeed, the extents of hypochromism, fluorescence quenching and energy transfer of (*S*)-TFAE upon binding to the double stranded polynucleotides were found to depend on the base pair sequence, suggesting a specific localization of the chromophore. Considering that CT-DNA is composed of 58% A–T base pairs and 42% G–C base pairs and that intercalation sites are only of the type GC–GC, AT–AT, and GC–AT, we calculate statistically that there are 33% AT–AT sites, 18% GC–GC sites and 49% AT–GC sites in CT-DNA. If hypochromism in absorption and fluorescence quenching were due to the proximity of (*S*)-TFAE to only one A–T base pair, then the extent of the effects should correspond to 82% of that measured with poly(dA-dT)-poly(dA-dT), which is not observed. It is inferred from the results obtained with CT-DNA [respectively 37% of absorption hypochromicity and 33% fluorescence quenching compared to (*S*)-TFAE–poly(dA-dT)-poly(dA-dT)] that the chromophore must be intercalated between two AT base pairs. This is also in agreement with the fact that the globally non polar TFAE chromophore may prefer intercalation into the less polar A–T sequences when compared to the more polar G–C sites.[34] The energy transfer data are consistent with this assumption though the extent of the fluorescence increase due to this process for the (*S*)-TFAE–CT-DNA complex is lower than expected. This could be explained by a less favorable relative orientation of the transition moments between the donor and the acceptor in the (*S*)-TFAE–CT-DNA complex compared to the (*S*)-TFAE–poly-(dA-dT)-poly(dA-dT) complex. The results can also be interpreted by considering the probability of having two successive A–T base pairs in CT-DNA: this probability is low and the energy transfer to the (*S*)-TFAE singlet state only occurs from the adjacent A–T bases while in poly(dA-dT)-poly(dA-dT), the energy transfer can originate from the A–T bases present in the Förster radius.

These results raise the question of the nature of the mechanism involved in this enantiospecificity of (*S*)-TFAE binding. From the single crystal X-ray studies of the chromophore[39] and the reasons for its ability to undergo enantiospecific separation,[40,41] one may suggest an intercalative model involving (*i*) the formation of a hydrogen bond OH · · · O between the OH of the asymmetric carbon of (*S*)-TFAE (Scheme 1) and the O^2 oxygen of the thymine of one A–T base pair; and (*ii*) an electrostatic interaction between the face of the chromophore opposite to the asymmetric carbon (which is electron deficient[38]) and a heteroatom of the second A–T base pair.

This model is supported by the following considerations. First a similar mechanism involving simultaneous occurrence of the two interactions cannot take place with (*R*)-TFAE due to the change of the enantiomer geometry around the chiral carbon, preventing the intercalation of this enantiomer. Second, this model can also explain why (*S*)-TFAE does not intercalate into poly(dG-dC)-(dG-dC). Indeed, in this polynucleotide, the O^2 oxygen of the cytosine is already implicated in a hydrogen bond with the H of the NH_2 group of the guanine.

Conclusion

Different modes of binding of TFAE to DNA may be distinguished readily by taking advantage of the different photophysical properties of each TFAE enantiomer. The experiments described here support the conclusion that each TFAE enantiomer binds to the B-DNA form but that significant enantiomeric discrimination of (*S*)- relative to (*R*)-TFAE occurs upon complexation. Furthermore, the results reveal that different local DNA structures and geometries may be recognized through binding by the chiral chromophore. Indeed, binding of (*R*)- and (*S*)-TFAE to poly(dG-dC)-poly(dG-dC) is negligible either by intercalation or surface binding, while (*S*)-TFAE intercalates specifically between two A–T base pairs and (*R*)-TFAE to the surface of natural CT-DNA. According to these results, each TFAE enantiomer can be used as a specific probe of the DNA sequence or topology.

Acknowledgements

We are grateful to Dr F. Lahmani and Dr A. Zehnacker-Rentien for helpful discussions. A. R. Al Rabaa gratefully acknowledges the Harii foundation for financial support. We are grateful to Dr M. Marden for the use of his fluorescence anisotropy apparatus.

References

1 J. Barton, L. Basile, A. Danishefsky and A. Alexandrescu, *Proc. Natl. Acad. Sci. USA*, 1983, **81**, 1961.
2 J. Barton, J. Goldberg, C. Kumar and N. Turro, *J. Am. Chem. Soc.*, 1986, **108**, 2081.
3 C. Hiort, P. Lincoln and B. Norden, *J. Am. Chem. Soc.*, 1993, **115**, 3448.
4 M. Barcena, G. Colmenarejo, M. Carmen Gutiérrez-Alonso, F. Montero and G. Orellana, *Biochem. Biophys. Res. Commun.*, 1995, **214**, 716.
5 N. Markoglou and I. Wainer, *J. Chromatogr.*, 1997, **693**, 493.
6 T. Fukushima, M. Kato, T. Santa and K. Imai, *Biomed. Chromatogr.*, 1995, **9**, 10.
7 H. Rau, *Chem. Rev.*, 1983, **83**, 535.
8 Y. Inoue, *Chem. Rev.*, 1992, **92**, 741.
9 W. Iwanek and J. Mattay, *J. Photochem. Photobiol. A*, 1992, **67**, 209.
10 T. Yorozu, K. Hayashi and M. Irie, *J. Am. Chem. Soc.*, 1981, **103**, 5480.
11 F. M. Pohl and T. M. Jovin, *J. Mol. Biol.*, 1912, **76**, 375.
12 R. D. Welles, J. E. Laarson, R. C. Grant, B. E. Shortle and C. R. Cantor, *J. Mol. Biol.*, 1970, **54**, 465.
13 S. J. Lippart, K. W. Jenette, H. C. Varsiliades and W. R. Bauer, *Proc. Natl. Acad. Sci. USA*, 1974, **71**, 3839.
14 M. P. Fontaine, L. Lindqvist, Y. Blouquit and J. Rosa, *Eur. J. Biochem.*, 1989, **186**, 663.
15 R. V. Bensasson, E. Land and T. G. Truscott, in *Excited states and free radicals in biology and medicine*, Oxford University Press, 1993, p. 80.
16 I. B. Berlmann, *Handbook of fluorescence spectra of aromatic molecules*, Academic Press, New York and London, 1971.
17 D. V. O'Connor and D. Phillips, in *Time correlated single photon counting*, Academic Press, London, 1984.
18 D. Deville-Bonne, O. Sellam, F. Merola, I. Lascu, M. Desmadril and M. Véron, *Biochemistry*, 1996, **35**, 14643.
19 P. Blandin, F. Mérola, J. C. Brochon, O. Trémeau and A. Ménez, *Biochemistry*, 1994, **33**, 2610.
20 W. W. Davis, M. E. Krahl and G. H. A. Clowes, *J. Am. Chem. Soc.*, 1942, **64**, 108.
21 K. Rohatgi, K. Bhattacharyya and P. Das, *J. Chem. Soc., Faraday Trans.*, 1985, **81**, 1331.
22 C. V. Kumar and E. Asuncion, *J. Am. Chem. Soc.*, 1993, **115**, 8547.

23 C. Kumar, J. Barton and N. Turro, *J. Am. Chem. Soc.*, 1985, **107**, 5518.
24 R. D. Ludescher, L. Peting, S. Hudson and B. Hudson, *Biophys. Chem.*, 1987, **28**, 59.
25 J. P. Morgan and M. Daniels, *Photochem. Photobiol.*, 1980, **31**, 101.
26 J.-L. Mergny, G. Duval-Valentin and C. Hélène, *Science*, 1992, **256**, 1681.
27 D. Pilch, M. J. Waring, J.-S. Sun, E. Bisagni and C. Hélène, *J. Mol. Biol.*, 1993, **232**, 926.
28 M. Daniels, in *Physico-Chemical properties of nucleic acids*, vol. 1, ed. J. Duchesne, Academic Press, New York, 1973, p. 99.
29 C. R. Cantor and P. R. Schimmel, in *Biophysical Chemistry*, *Part II: techniques for the study of biological structure and function*, Freeman, New York, 1980, p. 452.
30 R. Bensasson and E. J. Land, *Trans. Faraday Soc.*, 1971, **67**, 1904.
31 E. M. Fielden and E. J. Hart, *Trans. Faraday Soc.*, 1967, **63**, 2975.
32 J. A. Delaire, M. Castella, J. Faure, P. Vanderauwera and F. C. de Schryver, *Nouv. J. Chim.*, 1984, **8**, 231.
33 E. Renault, M. P. Fontaine-Aupart, F. Tfibel, M. Gardès-Albert and E. Bisagni, *J. Photochem. Photobiol. B*, 1997, **40**, 218.
34 C. V. Kumar and E. H. Asuncion, *J. Chem. Soc.*, *Chem. Commun.*, 1992, 470.
35 E. Tuite and J. M. Kelly, *Biopolymers*, 1995, **35**, 419.
36 Y. Kubota, Y. Motoda, Y. Shigemune and Y. Fujisaki, *Photochem. Photobiol.*, 1979, **29**, 1099.
37 C. Knapp, J.-P. Lecomte, A. Kirsch-De Mesmaeker and G. Orellana, *J. Photochem. Photobiol. B*, 1996, **36**, 67.
38 M. Enescu and L. Lindqvist, *J. Phys. Chem.*, 1995, **99**, 8405.
39 M. Webb and H. Rzepa, *Chirality*, 1994, **6**, 245.
40 W. Pirkle and C. Boeder, *J. Org. Chem.*, 1977, **42**, **23**, 3697.
41 J. W. Christopher, *J. Chromatogr. A*, 1994, **666**, 3.

Paper 8/04824J